J. Fluid Mech. (1999), *vol.* 390, *pp.* 251–270. Printed in the United Kingdom

© 1999 Cambridge University Press

Increased mobility of a surfactant-retarded bubble at high bulk concentrations

By YANPING WANG[1], DEMETRIOS T. PAPAGEORGIOU[1], AND CHARLES MALDARELLI[2]

[1]Department of Mathematical Sciences, and Center for Applied Mathematics and Statistics, New Jersey Institute of Technology, Newark, NJ 07102, USA

[2]Levich Institute and Department of Chemical Engineering, City College of New York, Convent Avenue at 140th Street, New York, NY 10031, USA

(Received 5 January 1998 and in revised form 28 January 1999)

We study theoretically the adsorption of surfactant onto the interface of gas bubbles in creeping flow rising steadily in an infinite liquid phase containing surface-active agents. When a bubble rises in the fluid, surfactant adsorbs onto the surface at the leading edge, is convected by the surface flow to the trailing edge and accumulates and desorbs off the back end. This transport creates a surfactant concentration gradient on the surface that causes the surface tension at the back end to be lower than that at the front end, thus retarding the bubble velocity by the creation of a Marangoni force. In this paper, we demonstrate numerically that the mobility of the surfactant-retarded bubble interface can be increased by raising the bulk concentration of surfactant. At high bulk concentrations, the interface saturates with surfactant, and this saturation acts against the convective partitioning to decrease the surface surfactant gradient. We show that as the Péclet number (which scales the convective effect) increases, larger concentrations are necessary to remobilize the surface completely. These results lead to a technologically useful paradigm where the drag and interfacial mobility of a bubble can be controlled by the level of the bulk concentration of surfactant.

1. Introduction

When a droplet or gas bubble moves through a continuous liquid phase by the action of a driving force, surfactants dissolved in either the continuous or droplet phase adsorb onto the fluid particle interface. Frumkin & Levich (1947) (see also Levich 1962 and Edwards, Brenner & Wasan 1991) first constructed a framework by which this adsorption can retard the particle velocity. We describe this mechanism for the case in which surfactant is only in the continuous phase, with a far-field concentration C_∞. Surfactant adsorbed on the fluid particle surface is convected by the surface flow from the front to the particle's trailing end. The surface concentration increases causing kinetic desorption into the rear sublayer. (The sublayer is defined as the region of the bulk fluid immediately adjacent to the surface.) This desorption locally raises the sublayer concentration C_s, at the back above the bulk value C_∞, far from the interface. The difference drives a diffusive flux away from the trailing end. Similarly at the front end, the reduction in surface concentration causes kinetic adsorption from the front sublayer onto the front of the bubble. The front sublayer concentration decreases, creating a diffusive flux from the bulk to the front end.

https://doi.org/10.1017/S0022112099005157 Published online by Cambridge University Press

Eventually a steady state develops in which all these fluxes balance. The surface concentration at the trailing end is higher than that at the front, and the interfacial tension γ is lower at the back relative to the front. This interfacial tension difference creates a Marangoni stress along the surface which forces the front part of the surface to tug at the rear, reducing the interfacial mobility and at steady state increasing the drag for a given terminal velocity U.

There has been a long-standing theoretical interest in the Marangoni retardation of the interfacial and terminal velocities of buoyantly driven fluid particles due to adsorbed surfactant on the particle surface. This interest is motivated primarily by its relevance to the understanding of the performance of dropwise extraction and aeration processes (see, for example, Huang & Kintner 1989 and Beitel & Heideger 1971), where the reduction in interfacial mobility due to the presence of trace amounts of surfactant, or intentionally added surface-active species, reduces the interphase transfer. Recent microgravity applications have provided additional incentive for the study of this problem. In the absence of buoyancy, thermocapillary forces have been used to move fluid particles. The application of a temperature gradient to the continuous phase in which a fluid particle is situated creates a tension difference on the particle surface (since the tension decreases with increase in temperature) which drives the particle to the warmer end of the gradient. The retardation due to surfactant adsorption can reduce to near zero this thermocapillary velocity (Kim & Subramanian 1989*b*; Nadim & Borhan 1989 and Chen & Stebe 1997).

Using the Levich framework, several efforts have calculated, at steady state, the increase in drag for a particle moving at constant velocity due to the Marangoni forces created by the convective redistribution of surfactant along the surface. These investigations have examined two surfactant transport regimes. In the first, the rate of convection of surfactant along the surface is much faster than either the rates of bulk diffusion or kinetic exchange, so the surfactant behaves as if it were insoluble (to leading order in an asymptotic sense). In the second regime, kinetic and diffusive exchange are of the same order as surface convection, so transport in the continuous phase affects the surfactant gradient and Marangoni stress. We review the investigations in these two regimes below.

In the insoluble limit, kinetic and bulk exchange cannot match the convective rate. To scale the kinetic rate we use Langmuir kinetics,

$$\beta C_s(\Gamma_\infty - \Gamma) - \alpha\Gamma = j, \tag{1.1}$$

where α and β are the desorption and adsorption rate constants respectively, j is the kinetic flux, Γ is the surface concentration and Γ_∞ is the maximum packing concentration. For large bulk concentrations, the convective rate is of order $\Gamma_\infty Ua$, where U is the terminal velocity and a the particle radius. As the diffusive rate is of order DC_∞/a, where D is the bulk diffusion coefficient, the ratio of diffusive to convective rate can be written as $\chi_0 k/Pe$, where $k = \beta C_\infty/\alpha$, $\chi_0 = \alpha a/\beta\Gamma_\infty$ and Pe is the Péclet number defined as $Pe = Ua/D$. The ratio of kinetic desorption to surface convection is the Biot number, $B_i = \alpha a/U$. In the insoluble limit we have $\chi_o k/Pe \ll 1$ or $B_i \ll 1$. In both the buoyancy- and thermocapillary-driven applications, Péclet numbers tend to be large, and therefore diffusive limitations give rise to the insoluble limit when the bulk concentration of the surface-active species is small enough.

In the insoluble limit, when the surface Péclet number ($Pe_s = Ua/D_s$) is infinite, surfactant convected to the trailing end cannot diffuse back to the front. The surfactant forms a stagnant cap of angle ϕ at the back with zero interfacial velocity, while the front end is free of surfactant and therefore stress free. The drag increases with

https://doi.org/10.1017/S0022112099005157 Published online by Cambridge University Press

increasing ϕ. Several efforts have computed the dependence of the drag on ϕ for the case in which the inertia of the continuous liquid and particle phase (if the particle is a liquid) are negligible and the fluid particle is a sphere (viscous and inertial forces small compared to capillary forces). For buoyancy-driven motion, see Savic (1953), Griffith (1962), Harper (1973) (for small cap angles), and Davis & Acrivos (1966) for bubbles and Holbrook & Levan (1983*a*), Sadhal & Johnson (1982) and He, Maldarelli & Dagan (1991) for droplets, and for thermocapillary-driven motion of drops Kim & Subramanian (1989*b*). The size of the cap as a function of the bulk concentration of surfactant is obtained by an overall surfactant mass balance which requires that the net flux of surfactant to the surface equal zero at steady state (cf. Harper 1973 for the diffusion limited case and Sadhal & Johnson (1982) and He *et al.* (1991) for the kinetically determined case). The cap size and hence the drag increases as the bulk concentration increases. For bubble motion for which the fluid-phase inertia is not negligible (order-one Reynolds number, $Re = \rho Ua/\mu$, where ρ and μ are the continuous-phase density and viscosity, respectively), Bel Fdhila & Duineveld (1996) (for a spherical bubble shape) and McLaughlin (1996) (for a deformed shape) computed the drag for buoyancy-driven motion as a function of the cap angle, and the cap angle as a function of concentration for kinetic control. They demonstrated that at sufficiently large Re and cap angles, the immobility of the cap causes a recirculation at the back. Finally, in the insoluble limit, if the surface Péclet number is of order one, surfactant convected to the back can diffuse to the front end, spreading surfactant everywhere on the surface and reducing, at the same bulk concentration of surfactant, the Marangoni retardation relative to the infinite surface Péclet value, cf. for buoyancy-driven motion Holbrook & Levan (1983*b*) and Harper (1973) (for negligible inertia and a spherical geometry), and Leppinen, Renksizbulut & Haywood (1996*b*) (for order-one Re and fluid droplet deformation in air), and Kim & Subramanian (1989*b*) for thermocapillary-driven spherical bubbles with negligible inertia.

The insoluble-limit asymptotics described above has been confirmed numerically in the recent study of Cuenot, Magnaudet & Spennato (1996) of the buoyancy-driven motion of a spherical bubble at order-one Reynolds number. This investigation formulated and solved the convective diffusion equation at large surface and bulk Péclet numbers (5×10^4) and low bulk concentrations ($k = 0.112$ and 0.0112). In addition χ_0 was equal to 5 or 50, and hence $\chi_0 k/Pe \ll 1$. (Note that the kinetic exchange was also slow.) The simulation results illustrate a cap by the collection of surfactant at the back end (due to the high surface Péclet number), and confirm the formation of a wake at order-one Reynolds number as noted by Bel Fdhila & Duineveld (1996) and McLaughlin (1996).

In the second regime, surfactant transport from the bulk to the surface matches the convective transport. If the kinetic rate is fast relative to convection, the surface and sublayer are in equilibrium. Bulk diffusion then governs the surfactant transport (the convection/bulk diffusion regime), with the parameter $\chi_0 k/Pe$ of order one or larger in this regime, determining the bulk concentration distribution. All studies of the convection/bulk diffusion regime considered the case of a slightly soluble surfactant or a surfactant at low bulk concentration ($k \ll 1$). Several studies examined the case of large Péclet number, and used a boundary layer analysis to describe the diffusive flux, cf. Deryagin, Dukhin & Lisichenko (1959), Saville (1973), Levich (1962) and Harper (1974, 1982) for negligible inertia and a spherical particle, and Andrews, Fike & Wong (1988) for a deformed particle at order-one Reynolds number; all these studies are for buoyancy-driven motion. The first studies in the direction of solving

https://doi.org/10.1017/S0022112099005157 Published online by Cambridge University Press

the convective diffusion directly were Levan & Newman (1976) and Holbrook & Levan (1983*b*) for the case of buoyancy-driven motion of a spherical particle in the absence of inertia. Levan demonstrated that as the bulk concentration increases, the drag increases. This increase in drag follows from the fact that the concentration difference between the bulk and the sublayer increases with bulk concentration for $k \ll 1$, and this results in an increase in the surface concentration difference since the sublayer and surface are in equilibrium. Thus the gradient on the surface increases, and this accounts for the increase in drag.

The above studies at low bulk concentrations in the convection/bulk diffusion regime (the parameter $\chi_0 k/Pe$ of order one or larger and fast kinetics) leave open the question of the effect of increasing bulk concentration in this regime. From the above scaling arguments, we expect that at high bulk concentrations the concentration difference will become independent of the bulk concentration. This results from the fact that the equilibrium surface concentration saturates to Γ_∞ for $k \gg 1$, and the concentration difference required by diffusion to balance the convection of a saturated surface becomes constant. In addition because of this saturation at high bulk concentration, the bulk concentration difference creates a smaller surface concentration difference reflecting the fact that the isotherm becomes flat at high bulk concentration near saturation. Thus we might expect the Marangoni retardation to decrease at increasing bulk concentrations in the convection/bulk diffusion regime, a surprising result not anticipated from the low-concentration studies of Holbrook & Levan (1983*b*) in this regime, or the stagnant cap regime, both of which predict an increase in drag with k. The gradual removal of the Marangoni force at high concentration leads to a potentially useful paradigm in technological applications with high bulk and surface Péclet numbers: For low bulk concentrations in the high Péclet number regime, stagnant caps form, and the drag increases with concentration as the cap angle increases. However, for larger concentrations for which $\chi_0 k/Pe$ becomes of order one or larger, we enter the convection/bulk diffusion regime and the drag begins to decrease with concentration. At increasingly higher concentrations for which $\chi_0\, k/Pe \gg 1$, the interface mobility increases and returns to an unretarded state as the surface concentration gradients and Marangoni force disappear. Increasing the concentration then provides a measure of mobility control, bringing the interface from the stagnant cap regime to a completely remobilized regime.

The aim of this paper is to illustrate this mobility control through the numerical solution of a model problem. We consider a spherical gas bubble which rises steadily and axisymmetrically with velocity U by buoyancy in an infinite, incompressible, continuous, Newtonian fluid with a dissolved surfactant with uniform concentration far from the sphere. Surfactant adsorption will be described by the Langmuir formulation. Since the mechanism of relaxation of the Marangoni stress is independent of the continuous-phase inertia, we will examine the simpler case of creeping flow. In the convective/diffusion regime discussed above, kinetic exchange is fast relative to the rate of convection. If kinetic exchange is of the order of convection, then the surface concentration gradients will be larger, and the Marangoni stress greater than for infinite exchange. Thus in the limit of high concentration the Marangoni gradient will not relax completely, but a remaining gradient will be supported by the kinetic limitation. Studies in which no bulk concentration gradients are considered and only a kinetic limitation is retained do indicate that as the kinetic exchange increases the retardation decreases and eventually disappears, cf. Chen & Stebe (1996, 1997) for buoyancy- and thermocapillary-driven motions of spherical droplets. In order to establish the relaxation at high bulk concentration, in this study we will focus on the

https://doi.org/10.1017/S0022112099005157 Published online by Cambridge University Press

rapid kinetic limit for which the relaxation is most pronounced. Kinetic effects can easily be incorporated, but will not alter the relaxation mechanism. For this same reason, surface diffusion will be neglected relative to surface convection. This paper is organized as follows. In § 2, the transport equations are detailed, and the numerical algorithm for their solution is outlined. In § 3, simulations of the drag, interfacial velocity and bulk and surface concentrations are presented as a function of the bulk concentration to illustrate the remobilization regime. Finally in the last section, we conclude with a discussion comparing the results obtained to experiments undertaken in the literature.

2. Mathematical model and numerical method

2.1. *Mathematical model*

The field equations for the flow and surfactant transport for a bubble rising steadily and axisymmetrically in creeping flow through a incompressible, Newtonian continuous phase containing surfactant is described by the Stokes and convection–diffusion equations. By the nature of the problem, it is most convenient to formulate these equations in spherical coordinates (r, θ, ϕ), fixed to the bubble (and centred at the bubble origin), with $\theta = 0$ representing the upstream direction. We examine the system of equations in non-dimensional form, where we non-dimensionalize the velocity by the free-stream (or bubble) velocity U, the length by the bubble radius a, and the concentration by the bulk concentration at infinity C_∞. Since the flow is axisymmetric and the fluid is incompressible, the solution is independent of the azimuthal angle ϕ, the velocity field can be written in terms of the stream function ψ:

$$u_r = -\frac{1}{r^2 \sin\theta}\frac{\partial \psi}{\partial \theta}, \quad u_\theta = \frac{1}{r \sin\theta}\frac{\partial \psi}{\partial r}, \tag{2.1}$$

and the vorticity has only one component w in the azimuthal direction. The Stokes equations are most conveniently expressed in terms of the stream function and vorticity in the form

$$\frac{\partial w}{\partial t} = \mathrm{E}^2(rw \sin\theta), \tag{2.2}$$

$$rw = \mathrm{E}^2\psi, \tag{2.3}$$

where

$$\mathrm{E}^2 = \frac{1}{\sin\theta}\frac{\partial^2}{\partial r^2} + \frac{1}{r^2}\frac{\partial}{\partial \theta}\left(\frac{1}{\sin\theta}\frac{\partial}{\partial \theta}\right). \tag{2.4}$$

The surfactant transport in the bulk is expressed by the convection–diffusion equation

$$\frac{\partial C}{\partial t} + \boldsymbol{u} \cdot \nabla C = \frac{1}{Pe}\nabla^2 C, \tag{2.5}$$

where, as before, $Pe = Ua/D$ is the Péclet number, with D being the diffusion coefficient.

The boundary conditions at the axes of symmetry are

$$\psi = 0, \qquad w = 0, \qquad \frac{\partial C}{\partial \theta} = 0 \qquad \text{at} \qquad \theta = 0, \pi, \tag{2.6}$$

https://doi.org/10.1017/S0022112099005157 Published online by Cambridge University Press

and the zero normal velocity at the interface leads to

$$\psi = 0 \qquad \text{at} \qquad r = 1. \tag{2.7}$$

Surfactant molecules adsorbing onto the bubble surface are transported by convection and diffusion along the interface. The surfactant interfacial conservation without surface deformation is described by the equation (neglecting surface diffusion)

$$\frac{\partial \Gamma}{\partial t} + \frac{1}{\sin\theta}\frac{\partial}{\partial \theta}(u_\theta \Gamma \sin\theta) = \frac{\chi_0 k}{Pe}\left.\frac{\partial C}{\partial r}\right|_{r=1}, \tag{2.8}$$

where Γ is the surface concentration non-dimensionalized by the maximum packing density of surfactant Γ_∞ (as introduced in § 1) $\chi_0 = a\alpha/\beta\Gamma_\infty$, and $k = \beta C_\infty/\alpha$ is the measure of the bulk concentration (α and β are the (Langmuir) desorption and adsorption rate constants respectively).

The presence of the surfactants creates a surface tension gradient and causes a force on the bubble surface that must be compensated by a viscous tangential stress on the interface. This is expressed as

$$\frac{1}{a}\frac{\partial \gamma}{\partial \theta} = -\tau_{r\theta}|_{r=1}, \tag{2.9}$$

where $\tau_{r\theta}$ is the shear stress, and γ is the surface tension. Combining this with the equation of state derived from Langmuir adsorption (see Levich 1962)

$$\gamma = \gamma_c + RT\Gamma_\infty \ln(1-\Gamma) \tag{2.10}$$

we have

$$\tau_{r\theta}|_{r=1} = \frac{Ma}{1-\Gamma}\frac{\partial \Gamma}{\partial \theta}, \tag{2.11}$$

where $Ma = RT\Gamma_\infty/\mu U$ is the Marangoni number, μ is the viscosity, R is the gas constant and T is the temperature.

The stress balance leads to a boundary condition for the vorticity at the surface

$$w = \frac{2}{\sin\theta}\frac{\partial \psi}{\partial r} + \frac{Ma}{1-\Gamma}\frac{\partial \Gamma}{\partial \theta}. \tag{2.12}$$

In this paper we assume that kinetics is fast relative to convection. In non-dimensional form the Langmuir kinetic scheme becomes

$$\frac{\chi_0 k}{Pe}\frac{\partial C}{\partial r} = B_i(kC_s(1-\Gamma) - \Gamma) \quad \text{at} \quad r = 1. \tag{2.13}$$

For fast adsorption and desorption (diffusion-controlled transport), $B_i \gg 1$ and therefore in order for the diffusive rate to be finite we must have

$$\Gamma = \frac{kC_s}{1+kC_s}, \tag{2.14}$$

where C_s is the bulk concentration at the surface. Equation (2.14) therefore defines thermodynamic equilibrium between the sublayer and the surface.

At infinity, the boundary conditions match to the free-stream and uniform concentration:

$$\psi = \tfrac{1}{2}r^2\sin^2\theta, \quad w = 0, \quad c = 1. \tag{2.15}$$

In general, the nonlinear system (2.2), (2.3) and (2.5) coupled with the boundary conditions (2.6), (2.7), (2.8), (2.14) and (2.15) cannot be solved analytically. We will solve for the steady state by using the following numerical method.

https://doi.org/10.1017/S0022112099005157 Published online by Cambridge University Press

2.2. *Numerical algorithm*

We use a finite-difference method along with ADI time discretizations (Alternating Directions Implicit method) for the pseudo-unsteady system which is widely used in fluid dynamics (see Peyret & Taylor 1983). The ADI scheme splits each time step into two steps. As a result, only tridiagonal systems of linear algebraic equations need to be solved, and the method is second-order accurate. Alternatively the nonlinear steady-state problem can be addressed directly and the resulting algebraic equations solved by iteration (for example SOR or conjugate gradient methods – see Peyret & Taylor 1983).

With the finite-difference method, one has to limit the radial direction at some finite radius r_∞. Applying the uniform-stream boundary condition directly at infinity on $r = r_\infty$ would introduce an error, and the proper way to minimize this error is to obtain a correction term for the stream function as $r \to \infty$ (see Happel & Brenner 1962), and use the corrected stream function as the boundary condition at the finite radius r_∞. The result is

$$\psi = \tfrac{1}{2}r^2 \sin^2\theta + \tfrac{1}{8}F_D r \sin^2\theta \quad \text{as } r \to \infty \tag{2.16}$$

for creeping flow, where F_D is the total drag on the particle non-dimensionalized by $\pi\mu Ua$. We found that the drag on the particle is about 6% higher if we apply the uniform-stream condition directly on $r = r_\infty$ than that with the correction term. Secondly, discretizing the equations directly on the physical domain would give an expanding mesh as r increases. To avoid this problem we transform the physical domain (r, θ) onto a unit square (x, y) using $r = r_\infty^x$ and $\theta = \pi y$.

To check if the code works correctly, we used it to solve limiting problems for which analytical solutions exist, and compared the analytical solutions with the predicted numerical results. We found two analytically solvable problems. These solutions describe unsteady adsorption of surfactant from a spatially uniform state to an initially clean bubble surface, with no flow where the surface is either an infinite sink for surfactant ($C_s = 0$) or the adsorption is linear $\Gamma = kC_s$. The solutions for the concentration fields are, respectively,

$$C = 1 - \frac{1}{r} + \frac{1}{r}\mathrm{erf}\left(\frac{r-1}{2\sqrt{tPe}}\right) \tag{2.17}$$

and

$$C = 1 - \frac{k}{\pi r}\int_0^\infty \frac{\chi\sqrt{y}\cos\sqrt{y}(r-1) + (\chi - ky)\sin\sqrt{y}(r-1)}{(\chi - ky)^2 + \chi^2 y}\mathrm{e}^{-ytPe}\,\mathrm{d}y, \tag{2.18}$$

where $\chi = \chi_0 k$. Agreement between numerical solutions and the solutions above is excellent.

As an additional accuracy test for the numerics, we developed an asymptotic solution for the steady drag F_D (non-dimensionalized by $\pi\mu Ua$) for the full problem for $k \ll 1$ (small bulk concentration) and $Pe = O(k)$, see the Appendix. In this case the drag is given by

$$F_D = -4 - \frac{2QMa}{3\chi_0}k^2 + \frac{4QMa}{3\chi_0}k^3 + \cdots, \tag{2.19}$$

where $Pe = Qk$, with Q a constant measuring the size of Pe. We found that the difference between asymptotic and numerical solutions was less than 0.5%.

Finally, we also computed the non-dimensional steady surfactant mass transfer (the Nusselt number) for a spherical bubble rising in creeping flow (as given by

https://doi.org/10.1017/S0022112099005157 Published online by Cambridge University Press

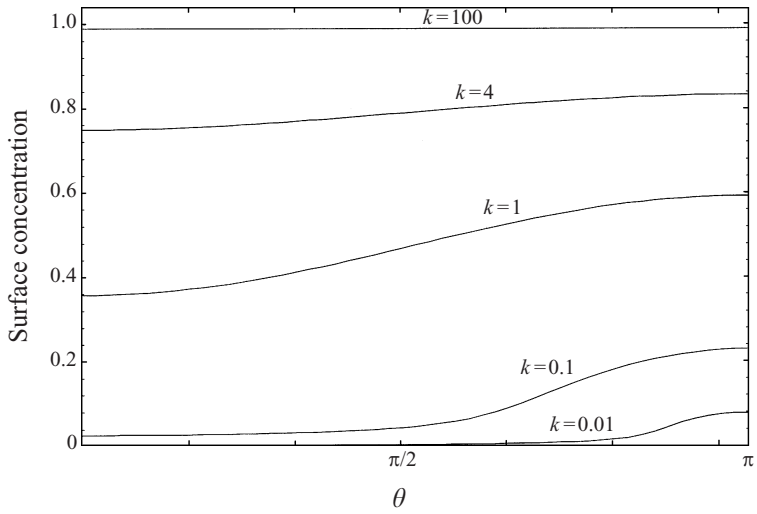


FIGURE 1. The surface concentration distribution, for $Ma = 5$, $\chi_0 = 1$ and $Pe = 10$. $\theta = 0$ is the leading edge and $k = \beta C_\infty/\alpha$ is the bulk concentration.

the Hadamard–Rybczynski velocity field) for $C_s = 0$ with order-one Péclet number ($Pe = 3, 10, 40, 70$), and found excellent agreement with Masliyah & Epstein's (1971) numerical result for the Nusselt number.

3. Results

The results were computed on a 50×50 grid and the time steps were 2×10^{-2} for most of the calculations. However, for $k = 100$, since bulk diffusion is much faster (relative to convection) than for smaller k and the surface concentration becomes almost uniform, equation (2.8) becomes stiff and the time step has to be reduced accordingly (see Peyret & Taylor 1983 for details). The criterion of convergence for the results is $\max|\psi_{n+100} - \psi_n| < 10^{-6}$, with n being the nth time step. We also checked a few results on a 100×100 grid, and found that the drag F_D on a 100×100 grid is 0.3% higher.

To illustrate remobilization, we calculate the results by varying the concentration k and Péclet number Pe about a reference case having $Ma = 5$ and $\chi_0 = 1$. We plot the drag, surface concentration distribution and surface velocity profile, and the contour of bulk concentration to show that the bubble motion can be controlled by bulk concentration. All graphs presented in this Section depict dimensionless variables.

3.1. *Surface concentration distribution*

The surfactant adsorbs onto the particle surface at the leading edge, convects to the trailing edge by surface flow, and then diffuses into the bulk as the particle migrates in the fluid. The adsorption of the surfactant onto the liquid interface develops a gradient of surfactant on the surface. In figure 1, we plot the surface concentration distribution as a function of θ for $Pe = 10$ and various bulk concentrations k. The figure shows that for any k (bulk concentration), the surface concentration at the trailing edge ($\theta = \pi$) is higher than that at the leading edge ($\theta = 0$), and that as k increases the amount of surfactant adsorbed on the surface increases. As we discussed in the Introduction, for large Péclet number and small bulk concentration

https://doi.org/10.1017/S0022112099005157 Published online by Cambridge University Press

the convection on the surface is much larger than the diffusion to the bulk, which is evident also from equation (2.8), and surfactants accumulate at the back end to form a stagnant cap. This phenomenon is shown in the surface concentration distribution above for $k = 0.01$, where the front end is free of surfactant, while a sharp surface concentration gradient develops in a small region near the rear stagnant point. The cap size increases as concentration k increases, and eventually the cap covers the entire surface.

When the bulk concentration increases to about $k = 1$, the parameter $\chi_0 k/Pe$ increases and a surface concentration gradient develops on the entire sphere as surface convection and bulk diffusion become of the same order. As we increase the bulk concentration further to $k = 100$, the distribution of surfactant on the surface is almost uniform (the bubble surface has been remobilized) as the parameter $\chi_0 k/Pe$ becomes larger. This argument readily follows from the surface concentration conservation equation (2.8) and equation of equilibrium between the surface concentration and the sublayer (2.14). It follows from (2.14) that the amount of surfactant adsorbed onto the surface increases as the bulk concentration increases. From (2.8), as k increases the ratio of bulk diffusion to convection $\chi_0 k/Pe$ increases for fixed Péclet number.

3.2. *Bulk concentration distribution*

In figure 2, we plot the contours of concentration for $Pe = 10$, $Ma = 5$, and $\chi_0 = 1$ with varying k (0.1, 1, 10, 100). For $k = 0.1$, the concentration near the leading edge is much smaller than that near the trailing edge, and the sublayer concentration at the front end is almost uniform, as is the distribution for a near stagnant cap regime. As k increases to 1, and the parameter $\chi_0 k/Pe$ increases and becomes of order one, bulk diffusion balances surface convection and the sublayer concentration varies along the whole surface. As this parameter becomes much larger than one, the characteristic concentration difference relative to the bulk concentration tends to zero, and this is evident in the figure where for $k = 10$ and 100 the non-dimensional concentration is becoming uniform in the bulk.

3.3. *Surface velocity*

As a concentration gradient develops on the surface, a surface tension gradient develops that creates a Marangoni force in the opposite direction to the surface flow and reduces the surface velocity. But as shown in figure 1, the surface concentration becomes uniform as k increases for a fixed Péclet number. The reduction in the surface concentration gradient causes an increase in the surface mobility as is evident in figure 3 which plots the surface velocity as a function of θ and k with the same values of Ma, Pe and χ_0 as in figure 1. Note that for a clean interface, the surface velocity is equal to $\sin\theta/2$, so at any point on the surface the velocity cannot be larger than $\sin\theta/2$ for any k. That is exactly what is shown in figure 3. When the bulk concentration is small ($k = 0.01$ and 0.1), the surface velocity is the same as that for the clean surface near the leading edge ($\theta = 0$), but it is smaller near the rear stagnant point ($\theta = \pi$) which corresponds to the surface concentration gradient in figure 1. As k increases from 0 to 1, the surface velocity decreases from the clean value $\sin\theta/2$. This is the retardation in interfacial flow that is usually associated with surfactant adsorption. However as k increases further, the velocity increases, and at $k = 100$ the velocity profile tends to that for clean surface. This elevated concentration velocity profile is almost symmetric about $\theta = \pi/2$, since the bubble interface has been remobilized.

https://doi.org/10.1017/S0022112099005157 Published online by Cambridge University Press

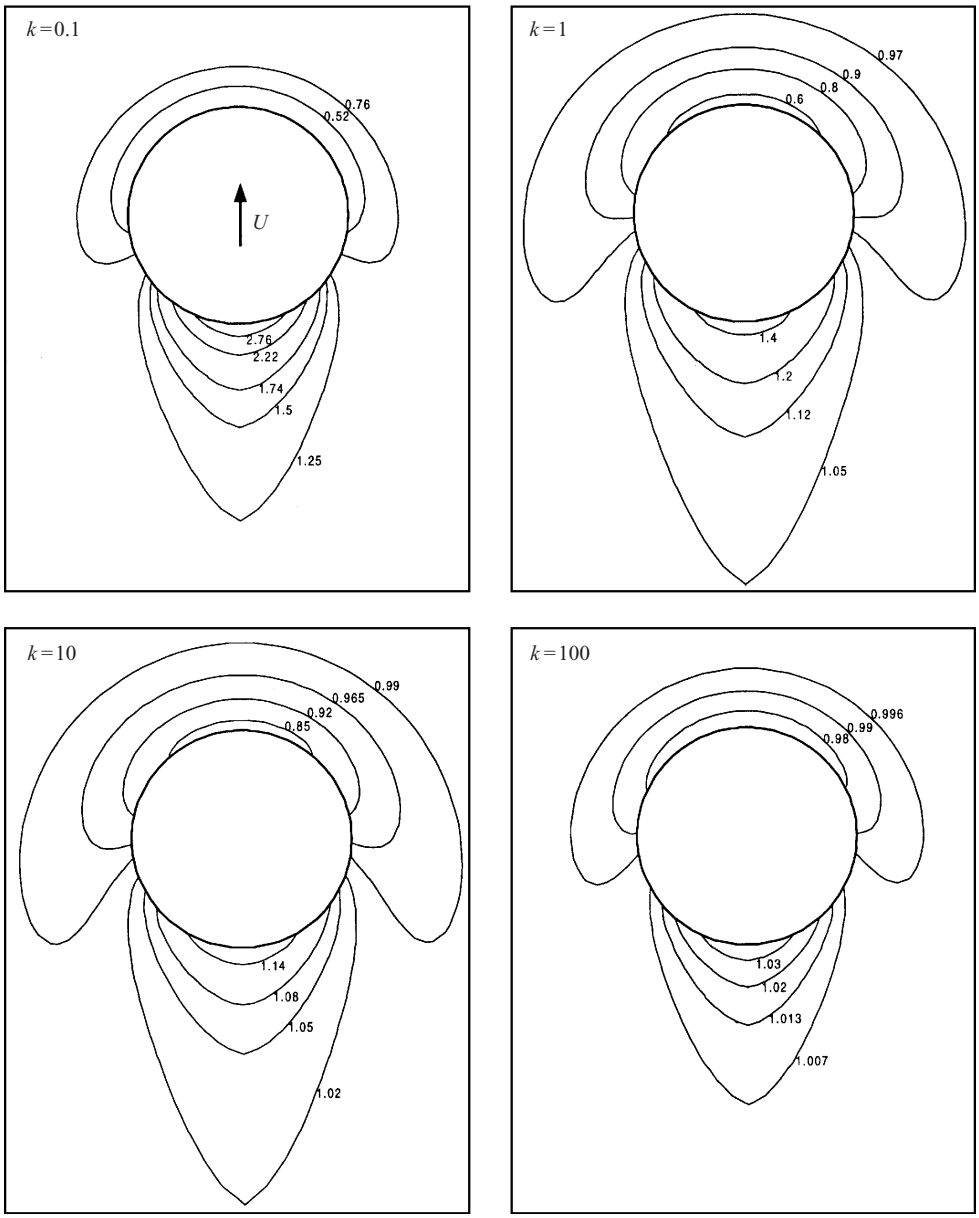


FIGURE 2. Contours of concentration, for $Ma = 5$, $\chi_0 = 1$ and $Pe = 10$. U is the terminal velocity and $k = \beta C_\infty/\alpha$ is the bulk concentration.

3.4. *Drag on the bubble*

The effect of bulk concentration on the terminal velocity is given in Figure 4 by examining the way the bubble drag non-dimensionalized by $\pi\mu aU$ is affected by the bulk concentration of surfactant. Three different Péclet numbers are used ($Pe = 0.1$, 1.0, and 10.0). In this non-dimensional unit, the drag on a clean bubble is 4 and the drag on a completely immobile surface (solid surface) is equal to 6. We found that, for a fixed Péclet number, as we vary the bulk concentration k from 0.01 to 100, the drag first increases monotonically as a function of concentration (corresponding to

https://doi.org/10.1017/S0022112099005157 Published online by Cambridge University Press

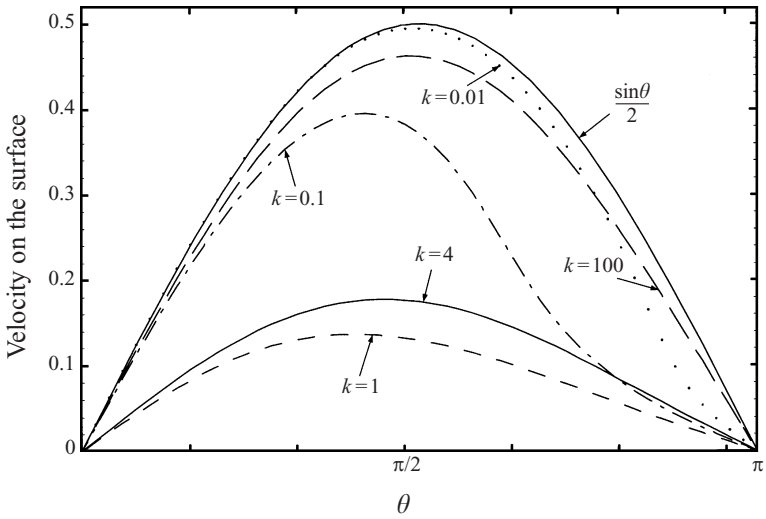


FIGURE 3. Velocity on the bubble surface, where $\sin\theta/2$ is the surface velocity for the clean surface, for $Ma = 5$, $Pe = 10$, and $\chi_0 = 1$. $\theta = 0$ is the leading edge and $k = \beta C_\infty/\alpha$ is the bulk concentration.

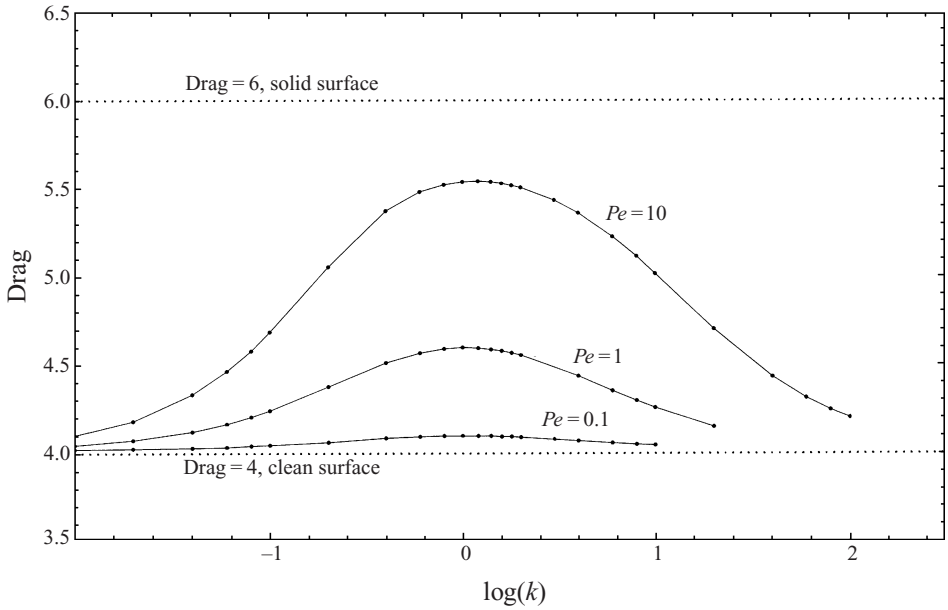


FIGURE 4. The effect of concentration on the drag, for $Ma = 5$ and $\chi_0 = 1$ and the dots are the actual points calculated. $\theta = 0$ is the leading edge and $k = \beta C_\infty/\alpha$ is the bulk concentration.

the decrease in the interfacial mobility observed in figure 3) when the concentration is small (= 0.01–1), but decreases to the clean-surface value when the concentration gets large as the interface remobilizes. With concentration fixed, as we vary the Péclet number from 0.1 to 10, the drag increases as the Péclet number increases. The larger the Péclet number is, the larger the concentration needs to be to bring the drag down to the clean-surface value, as shown in figure 4, where the calculations are for $Ma = 5$ and $\chi_0 = 1$.

https://doi.org/10.1017/S0022112099005157 Published online by Cambridge University Press

3.5. *Scaling argument explanation for remobilization*

We have argued that the increase in surface velocity and reduction in drag are due to the fact that the surface concentration becomes nearly uniform (and non-dimensionally equal to one) as the bulk concentration becomes large. The Marangoni force as given in equation (2.11) is $Ma/(1-\Gamma)(\partial\Gamma/\partial\theta)$. Therefore even though the surface concentration is becoming uniform ($\Gamma \to 1$), because of the singular part of the Marangoni force for Γ near 1, small concentration gradients can still give rise to order one or larger Marangoni forces. The remobilization obtained in the above numerical results for the surface velocity and drag reflect the fact that the concentration gradient on the surface tends to zero faster, as k becomes large, than the Marangoni stress diverges. We can use scaling arguments to verify the numerical results. The scale for the retarding Marangoni force is given by

$$\tau_m = \frac{\text{interfacial tension gradient}}{\text{viscous stress}} = O\left(\frac{1}{\mu U}\left[\frac{\partial\gamma}{\partial\Gamma}\right]_{\Gamma_0}\Delta\Gamma\right), \tag{3.1}$$

where τ_m is the non-dimensional retarding Marangoni force and $\Gamma_0 = \Gamma_\infty k/(1+k)$ is the equilibrium surface concentration. The derivative of the equation of state for Langmuir adsorption is

$$\left[\frac{\partial\gamma}{\partial\Gamma}\right]_{\Gamma_0} = -\frac{RT}{1-\Gamma_0/\Gamma_\infty}. \tag{3.2}$$

As we developed in the Introduction, the bulk characteristic concentration gradient is obtained by balancing the convection ($\Gamma_0 Ua$) and diffusion ($(D\Delta C/a)a^2$), and is given by

$$\frac{\Delta C}{C_\infty} = O\left(\frac{Pe}{\chi_0(1+k)}\right) \tag{3.3}$$

and therefore from adsorption equilibrium

$$\Delta\Gamma = O\left(\frac{k\Gamma_\infty Pe}{\chi_0(1+k)^3}\right) \tag{3.4}$$

and the non-dimensional Marangoni force is

$$O\left(Ma\frac{kPe}{\chi_0(1+k)^2}\right). \tag{3.5}$$

In the case in which $k \ll 1$, the concentration difference is of order k, the difference in surface concentrations is also of order k because of the linearity of the isotherm at small k and therefore the non-dimensional Marangoni force scales with k. This explains the increasing of the drag as k increases from zero, as is shown by our results and those of Holbrook & Levan (1983*b*).

In the limit of large k, the retardation scales as $MaPe/\chi_0 k$ and tends to zero; although, from the equation of state, $\left[\partial\gamma/\partial\Gamma\right]_{\Gamma_0}$ scales as k at saturation, since the surface concentration difference scales as k^{-2} the retarding force decreases as k^{-1}, overcoming the fact that the surface becomes more incompressible.

4. Conclusions and comparison with experiments

We have shown that the bubble interface can be remobilized by controlling the bulk concentration. The ratio of bulk diffusion to convection $k\chi_0/Pe$ plays a very important

https://doi.org/10.1017/S0022112099005157 Published online by Cambridge University Press

role in this problem. When $k\chi_0/Pe = O(1)$, a surface concentration gradient develops over the entire surface, the Marangoni force is large, and the bubble terminal velocity is significantly reduced. As $k\chi_0/Pe \gg 1$, although the total amount of surfactant adsorbed onto the surface increases, the surface concentration becomes uniform (we say the bubble interface remobilizes). Since the diffusion to the bulk is much larger than the convection on the surface (as is evident from equation (2.8)), surfactant will not accumulate at the back end as we showed in figure 1. Hence the stress Marangoni force disappears, the bubble regains the velocity of that for the clean surface. The larger the Péclet number, the larger the bulk concentration needed to remobilize the bubble interface as shown in figure 4.

There is a long history associated with the measurement of the effect of surfactants on the motion of bubbles and drops. The early efforts Garner & Skelland (1955), Elzinga & Banchero (1961), and Horton Fritsch & Kintner (1965) all studied drops. They observed the reduction of interfacial mobility and diminishment and shift (to the leading pole) of the circulation vortex in the drop with surfactant present in the system. Systematic and more quantitative studies of the effect of the bulk concentration of surfactant on the terminal velocity began with the measurements of Edge & Grant (1972) of the velocity of dichloroethane drops in water with sodium lauryl sulphate as the surfactant, and later the measurements of Yamamoto & Ishii (1987) of the rise velocity of air bubbles in water again with sodium lauryl sulphate, and of Bel Fdhila & Duineveld (1996) of air bubble velocities in water with Triton X-100, Brij 30 and sodium dodecyl sulphate as the surfactants. All these studies investigated bubbles or drops of the order of 0.1–1 cm. Because of the low viscosity of water, the bubbles or drops were deformed and terminal velocities were of the order of 10 cm s^{-1}. Measurements were made of the terminal velocity as a function of increasing bulk concentration, at concentrations below the point at which micellar aggregates form in the bulk. All studies showed a decrease in velocity, with the expanded studies Edge & Grant (1972) and Bel Fdhila & Duineveld (1996) demonstrating that at high enough concentrations the velocity becomes constant with increasing concentration. The fact that the remobilization was not observed in these experiments is because the parameter $k\chi_0/Pe$ was probably much less than one, and the saturation in velocity may be due to a completely immobile interface. For the velocities and bubble and drop diameters used, Péclet numbers are of order 10^6–10^7, assuming 10^{-6} cm s^{-2} for the surfactant diffusion coefficient (The review article by Chang & Franses (1995) provides characteristic values for diffusion coefficients.) Also from tabulated literature values given in Chang & Franses (1995), we can estimate for the surfactants used χ_0 to be of order 1–10^2 and k between 1–10^3 . Thus irrespective of any kinetic constraints, the high Péclet numbers require the surfactant transport to be in the stagnant cap regime.

The above recent measurements point to the fact that the regime in which remobilization at increasing bulk concentration can be observed must be at low velocities and small fluid particles where Péclet numbers are necessarily smaller. The mechanism of remobilization outlined here is not limited to isolated drops or bubbles, but is valid for any fluid particles moving through a continuous phase. In this regard, the experiments of Stebe, Lin & Maldarelli (1991) provide strong evidence for the remobilization theoretically studied in this study. These authors studied a three-phase periodic slug flow in a capillary tube in which a train of alternating air and aqueous segments (containing the surfactant Triton X-100 or Brij 35) ride on an annular wetting film of flourocarbon oil. The surfactant adsorbs onto the oil/aqueous interface, where it is convected to the trailing edge of the slug. Slug velocities were of the order of 1 cm s^{-1}, and the viscosity of the oil was 5 g cm^{-1} s^{-1}. At low concentrations of

https://doi.org/10.1017/S0022112099005157 Published online by Cambridge University Press

the surfactant the pressure required to drive the slug train at a constant velocity was found to increase with the bulk concentration. However at high concentrations the pressure relaxed, indicating remobilization. In this case, the slower velocity of the slugs, and the higher viscosity of the oil allowed diffusion to outscale convection and remobilize the surface. In this study complete remobilization was only achieved in the limit of high concentrations where micelle aggregates formed in the bulk. Breakdown and reforming of these aggregates provides a second mechanism for maintaining a uniform surface concentration. The onset of micellization is the point at which k can no longer increase (after micelles form, the bulk concentration is sensibly constant). Thus micellization would provide the only route for remobilization when, because of elevated Péclet numbers, the parameter $k\chi_0/Pe$ cannot be made large by increase in bulk concentration.

This work was supported by a grant from NASA's Microgravity Fluid Physics, NAG 3 1618 to C.M. and D.T.P. and a National Science Foundation Grant DMS-970493 to D.T.P.

Appendix. Analytical solution for small bulk concentration and Péclet number

The objective of this Appendix is the asymptotic evaluation of the drag F_D experienced by the bubble in the limit of small bulk concentration k and small Péclet number of $O(k)$. It turns out that the $O(k)$ correction is zero and the asymptotic development is taken to $O(k^3)$ in order to provide an accurate enough result to compare with the simulations.

The exact system to be solved is

$$\left.\begin{aligned} &\mathrm{E}^4\psi = 0, \\ &\psi|_{r=1} = 0, \quad \psi|_{\theta=0,\pi} = 0, \quad \psi = \tfrac{1}{2}r^2\sin^2\theta\big|_{r\to\infty}, \\ &\psi_{rr} - 2\psi_r|_{r=1} = \frac{Ma}{1-\Gamma}\frac{\partial\Gamma}{\partial\theta}\sin\theta, \end{aligned}\right\} \tag{A 1}$$

for the hydrodynamics and

$$\left.\begin{aligned} &\boldsymbol{u}\cdot\nabla C = 1/Pe\nabla^2 C, \\ &\frac{1}{\sin\theta}\frac{\partial}{\partial\theta}(\sin\theta u_\theta\Gamma) = \frac{\chi k}{Pe}\frac{\partial C}{\partial r}\bigg|_{r=1}, \\ &\Gamma = \frac{kC_s}{1+kC_s} \quad \text{at} \quad r=1, \\ &C = 1 \quad \text{as} \quad r\to\infty, \end{aligned}\right\} \tag{A 2}$$

for the convection–diffusion equation governing the concentration distribution in the bulk. It can be seen from equation (A 2) that in the limit $k \ll 1$ (here we also take $Pe = Qk$ with Q a constant) the hydrodynamics decouples from the concentration dynamics, to leading order. In addition, at higher order this remains the case and forced versions of equation (A 1) need to be addressed.

Formally, then, we expand dependent variables in powers of k,

$$\psi = \psi_0 + k\psi_1 + k^2\psi_2 + k^3\psi_3 + \cdots, \tag{A 3}$$

$$\Gamma = \Gamma_0 + k\Gamma_1 + k^2\Gamma_2 + k^3\Gamma_3 + \cdots, \tag{A 4}$$

https://doi.org/10.1017/S0022112099005157 Published online by Cambridge University Press

$$C = C_0 + kC_1 + k^2C_2 + k^3C_3 + \cdots, \tag{A 5}$$

$$\boldsymbol{u} = \boldsymbol{u}_0 + k\boldsymbol{u}_1 + k^2\boldsymbol{u}_2 + k^3\boldsymbol{u}_3 + \cdots, \tag{A 6}$$

and substitute into (A 1) and (A 2), to obtain a sequence of problems at successive orders. The leading-order problem is

$$\left.\begin{aligned} &\mathrm{E}^4\psi_0 = 0, \\ &\psi_0|_{r=1} = 0, \quad \psi_0|_{\theta=0,\pi} = 0, \quad \psi_0|_{r\to\infty} = \tfrac{1}{2}r^2\sin\theta, \\ &\frac{\partial^2\psi_0}{\partial r^2} - \frac{\partial\psi_0}{\partial r}\bigg|_{r=1} = \frac{Ma\sin\theta}{1-\Gamma_0}\frac{\partial\Gamma_0}{\partial\theta}, \end{aligned}\right\} \tag{A 7}$$

and

$$\left.\begin{aligned} &\nabla^2 C_0 = 0, \\ &\frac{1}{\sin\theta}\frac{\partial}{\partial\theta}(\sin\theta u_{0\theta}\Gamma_0) = \frac{\chi}{Q}\frac{\partial C_0}{\partial r}\bigg|_{r=1}, \\ &\Gamma_0 = 0, \\ &C_0|_{r\to\infty} = 1. \end{aligned}\right\} \tag{A 8}$$

From (A 8) we have $\Gamma_0 = 0$, and the boundary conditions involving Γ_0 for (A 7) and (A 8) become, respectively,

$$\frac{\partial^2\psi_0}{\partial r^2} - \frac{\partial\psi_0}{\partial r}\bigg|_{r=1} = 0, \qquad \frac{\partial C_0}{\partial r}\bigg|_{r=1} = 0. \tag{A 9}$$

The hydrodynamics decouples, leading to the well-known Hadamard–Rybczynski solution (see for example Happel & Brenner 1962)

$$\psi_0 = \tfrac{1}{2}(r^2 - r)\sin^2\theta. \tag{A 10}$$

The general solution of (A 8) is $C_0 = \sum_{n=0}^{\infty} a_n r^{-n} P_n(\cos\theta)$ and application of the boundary condition at infinity gives $a_0 = 1$, while the boundary condition at the bubble surface implies $a_i = 0$ for $i = 1, 2, \cdots$. Thus, the leading-order solution for the concentration is

$$C_0 = 1. \tag{A 11}$$

At the next order, $O(k)$, the problem is

$$\left.\begin{aligned} &\mathrm{E}^4\psi_1 = 0, \\ &\psi_1|_{r=1} = 0, \quad \psi_1|_{\theta=0,\pi} = 0, \quad \psi_1|_{r\to\infty} = 0, \\ &\frac{\partial^2\psi_1}{\partial r^2} - \frac{\partial\psi_1}{\partial r}\bigg|_{r=1} = Ma\sin\theta\frac{\partial\Gamma_1}{\partial\theta}, \end{aligned}\right\} \tag{A 12}$$

and

$$\left.\begin{aligned} &\nabla^2 C_0 = 0, \\ &\frac{1}{\sin\theta}\frac{\partial}{\partial\theta}(\sin\theta u_{0\theta}\Gamma_1) = \frac{\chi}{Q}\frac{\partial C_1}{\partial r}\bigg|_{r=1}, \\ &\Gamma_1 = 1, \\ &C_1|_{r\to\infty} = 0, \end{aligned}\right\} \tag{A 13}$$

https://doi.org/10.1017/S0022112099005157 Published online by Cambridge University Press

where $u_{0\theta}|_{r=1} = (1/\sin\theta)(\partial\psi_0/\partial r) = \frac{1}{2}\sin\theta$ follows from the leading-order solutions. Since $\Gamma_1 = 1$ the boundary conditions involving Γ_1 in (A 12) and (A 13) become

$$\left.\frac{\partial^2\psi}{\partial r^2} - 2\frac{\partial\psi}{\partial r}\right|_{r=1} = 0 \text{ and } \left.\frac{\partial C_1}{\partial r}\right|_{r=1} = \frac{Q}{\chi}\cos\theta.$$

Thus, the solutions for (A 12) and (A 13) are

$$\psi_1 = 0, \tag{A 14}$$

$$C_1 = -\frac{Q}{2\chi}\frac{\cos\theta}{r^2}. \tag{A 15}$$

At $O(k^2)$ the problem is

$$\left.\begin{aligned} &\mathrm{E}^4\psi_2 = 0, \\ &\psi_2|_{r=1} = 0, \quad \psi_2|_{\theta=0,\pi} = 0, \quad \left.\frac{\psi_2}{r^2}\right|_{r\to\infty} = 0, \\ &\left.\frac{\partial^2\psi_2}{\partial r^2} - 2\frac{\partial\psi_2}{\partial r}\right|_{r=1} = Ma\sin\theta\frac{\partial\Gamma_2}{\partial\theta}, \end{aligned}\right\} \tag{A 16}$$

and for the concentration field,

$$\left.\begin{aligned} &\nabla^2 C_2 = Q\left(u_{0r}\frac{\partial C_1}{\partial r} + \frac{u_{0\theta}}{r}\frac{\partial C_1}{\partial\theta}\right), \\ &C_2|_{r\to\infty} = 0, \quad \Gamma_2 = C_{1s} - \Gamma_1 C_{0s}, \\ &\frac{1}{\sin\theta}\frac{\partial}{\partial\theta}(\sin\theta u_{0\theta}\Gamma_2) = \left.\frac{\chi}{Q}\frac{\partial C_2}{\partial r}\right|_{r=1}. \end{aligned}\right\} \tag{A 17}$$

The general solution for ψ_2 is $\psi_2 = \Sigma_{n=0}^{\infty}(A_n r^{-n+1} + B_n r^{-n+3} + C_n r^{n+2} + D_n r^n)C_n^{-1/2}(\cos\theta)$ where $C_n^{-1/2}(x)$ are the Gegenbauer polynomials (see Happel & Brenner 1962), and application of the first two boundary conditions of (A 16) gives

$$\psi_2 = \sum_{n=2}^{\infty} A_n(r^{-n+1} - r^{-n+3})C_n^{-1/2}(c), \tag{A 18}$$

where $c = \cos(\theta)$. Using this solution along with the known expression for Γ_2 (see (A 17) and (A 15)) provides the following equation connecting the unknown constants A_n:

$$\frac{QM_a}{2\chi}\sin^2\theta = 2\sum_{n=2}^{\infty}(2n-1)A_n C_n^{-1/2}(c) \tag{A 19}$$

from which it follows (using the properties of the Gegenbauer polynomials) that $A_2 = \frac{1}{6}QMa/\chi$, $A_n = 0$ otherwise. Hence,

$$\psi_2 = \frac{QMa}{12\chi}\left(\frac{1}{r} - r\right)\sin^2\theta. \tag{A 20}$$

Next, with ψ_0 and C_1 known, the concentration C_2 in (A 17) satisfies

$$\nabla^2 C_2 = \frac{Q^2}{\chi}\left[\cos^2\theta\left(\frac{1}{r^4} - \frac{1}{r^3}\right) + \sin^2\theta\left(\frac{1}{2r^3} - \frac{1}{3r^4}\right)\right]. \tag{A 21}$$

https://doi.org/10.1017/S0022112099005157 Published online by Cambridge University Press

Seeking a solution of the form

$$C_2(r,\theta) = \sum_{n=0}^{\infty} f_n(r) P_n(c), \tag{A 22}$$

where $c = \cos(\theta)$ as before, we find that the unknown functions $f_n(r)$ satisfy

$$\frac{1}{r^2}\frac{\mathrm{d}}{\mathrm{d}r}(r^2 f_0') = \frac{Q^2}{6\chi r^4}, \tag{A 23}$$

$$\frac{1}{r^2}\frac{\mathrm{d}}{\mathrm{d}r}(r^2 f_2') - \frac{6}{r^2} f_2 = \frac{Q^2}{6\chi}\left(\frac{5}{r^4} - \frac{6}{r^3}\right), \tag{A 24}$$

$$\frac{1}{r^2}\frac{\mathrm{d}}{\mathrm{d}r}(r^2 f_n') - \frac{n(n+1)}{r^2} f_n = 0 \quad \text{for} \quad n \neq 0, 2. \tag{A 25}$$

The general solutions are

$$f_0 = \frac{Q}{12\chi r^2} - \frac{d_0}{r} + b_0, \tag{A 26}$$

$$f_2 = \frac{Q^2}{6\chi}\left(\frac{1}{r} - \frac{5}{4r^2}\right) + \frac{d_2}{r^3} + b_2 r^2, \tag{A 27}$$

$$f_n = b_n r^n + d_n r^{-(n+1)} \quad \text{for} \quad n \neq 0, 2, \tag{A 28}$$

and since $C_2 = 0$ as $r \to \infty$, we require $b_n = 0$ for all n. Hence the general solution for C_2 assumes the form

$$C_2 = \sum_{n=0}^{\infty} d_n r^{-(n+1)} P_n(c) + \frac{Q^2}{12\chi r^2} + \frac{Q^2}{6\chi}\left(\frac{1}{r} - \frac{5}{4r^2}\right) P_2(c), \tag{A 29}$$

and the constants d_n can be found by substitution into the surfactant concentration boundary condition in equation (A 17). The result is

$$d_0 = -\frac{Q^2}{6\chi}, \quad d_1 = \frac{Q}{2\chi}, \tag{A 30}$$

$$d_2 = \frac{Q^2}{12\chi}\left(1 + \frac{2}{\chi}\right), \quad d_n = 0 \quad \text{for} \quad n \geqslant 3, \tag{A 31}$$

which together with (A 29) determines C_2.

Finally we consider the $O(k^3)$ problems

$$\left.\begin{aligned} &\mathrm{E}^4\psi_3 = 0, \\ &\psi_3|_{r=1} = 0, \quad \psi_3|_{\theta=0,\pi} = 0, \quad \left.\frac{\psi_3}{r^2}\right|_{r\to\infty} = 0, \\ &\left.\frac{\partial^2\psi_3}{\partial r^2} - 2\frac{\partial\psi_3}{\partial r}\right|_{r=1} = Ma\sin\theta\frac{\partial\Gamma_3}{\partial\theta} + \Gamma_1\left(\frac{\partial^2\psi_2}{\partial r^2} - 2\frac{\partial\psi_2}{\partial r}\right), \end{aligned}\right\} \tag{A 32}$$

https://doi.org/10.1017/S0022112099005157 Published online by Cambridge University Press

and

$$\left.\begin{aligned} &\nabla^2 C_3 = Q\left(u_{0r}\frac{\partial C_2}{\partial r} + \frac{u_{0\theta}}{r}\frac{\partial C_2}{\partial \theta}\right), \\ &C_3 = 0 \quad \text{as} \quad r \to \infty, \\ &\Gamma_3 = C_{2s} - \Gamma_1 C_{1s} - C_{0s}\Gamma_2, \\ &\frac{1}{\sin\theta}\frac{\partial}{\partial\theta}[\sin\theta(u_{0\theta}\Gamma_3 + u_{2\theta}\Gamma_1)] = \frac{\chi}{Q}\frac{\partial C_3}{\partial r}\bigg|_{r=1}. \end{aligned}\right\} \tag{A 33}$$

The solution for ψ_3 has the same form as that for ψ_2. Writing $\psi_3 = \Sigma_{n=2}^{\infty} B_n(r^{-n+1} - r^{-n+3})C_n^{-1/2}(c)$, the coefficients B_n are determined by substitution into the last boundary condition of (A 32) and use of the solutions already found for Γ_1, Γ_2, C_1 and C_2 (note that these determine Γ_3 which enters into the boundary conditions). The solution, then, is found to be

$$\psi_3 = -\frac{QMa}{3\chi}\left(\frac{1}{r} - r\right)C_2^{-1/2}(c) - \frac{Q^2 Ma}{40\chi}\left(1 + \frac{4}{\chi}\right)\left(\frac{1}{r^2} - 1\right)C_3^{-1/2}(c), \tag{A 34}$$

with $c = \cos(\theta)$ as before. Our interest is in computing the drag up to and including $O(k^3)$, so the solution for C_3 is not required.

Letting the drag on the bubble be F_D, the limit considered here implies the expansion

$$F_D = D_0 + kD_1 + k^2 D_2 + k^3 D_3 + \cdots. \tag{A 35}$$

The total drag on the bubble is found by integration of the forces acting on the interface and since the flow is axisymmetric, the drag is the magnitude of the total force acting along the axis of symmetry and opposing the motion. The drag is (see Happel & Brenner 1962) (in what follows P is the pressure at the bubble surface)

$$\begin{aligned} F_D &= \int_0^{\pi}\left(\sin^2\theta\frac{\partial P}{\partial\theta} - 2\sin\theta\frac{\partial^2\psi}{\partial r^2}\right)\mathrm{d}\theta \\ &= \int_0^{\pi}\left(\sin\theta\frac{\partial^3\psi}{\partial r^3} - 6\sin\theta\frac{\partial\psi}{\partial r} - 2Ma\frac{\sin^2\theta}{1-\Gamma}\frac{\partial\Gamma}{\partial\theta}\right)\mathrm{d}\theta. \end{aligned} \tag{A 36}$$

Substitution of the solutions ψ_0, ψ_1, ψ_2, ψ_3, Γ_2 and Γ_3 given above determines the coefficients in the expansion (A 35) for the drag,

$$D_0 = -4, \quad D_1 = 0, \quad D_2 = -\frac{QMa}{2\chi}\int_0^{\pi}\sin^3\theta\mathrm{d}\theta, \tag{A 37}$$

$$D_3 = \frac{2QMa}{\chi}\int_0^{\pi} C_2^{-1/2}(c)\sin\theta\mathrm{d}\theta + \frac{4Q^2 Ma}{5\chi}\left(1 + \frac{4}{\chi}\right)\int_0^{\pi} C_3^{-1/2}(c)\sin\theta\mathrm{d}\theta. \tag{A 38}$$

Using the result

$$\int_{-1}^{1} C_n^{-1/2}(\cos\theta)\mathrm{d}x = \left\{\begin{array}{ll} 2 & \text{if } n = 0, \\ \frac{2}{3} & \text{if } n = 2, \\ 0 & \text{otherwise,} \end{array}\right\} \tag{A 39}$$

gives the asymptotic result (2.19) used in § 2.2.

https://doi.org/10.1017/S0022112099005157 Published online by Cambridge University Press

REFERENCES

Acrivos, A. & Goddard, J. D. 1965 Asymptotic expansions for laminar forced-convection heat and mass transfer. *J. Fluid Mech.* **23**, 273–291.

Andrews, G. F., Fike, R. & Wong, S. 1988 Bubble hydrodynamics and mass transfer at high Reynolds number and surfactant concentration *Chem. Engng Sci.* **43**, 1467–1477.

Barton, K. D. & Subramanian, R. S. 1989 The migration of liquid drops in a vertical temperature gradient. *J. Colloid Interface Sci.* **133**, 211–222.

Beitel, A. & Heideger, W. J. 1971 Surfactant effects on mass transfer from drops subject to interfacial instability. *Chem. Engng Sci.* **26**, 711–717.

Bel Fdhila, R. & Duineveld, P. C. 1996 The effect of surfactants on the rise of a spherical bubble at high Reynolds and Péclet numbers. *Phys. Fluids* **8**, 310–321.

Chang, C.-H. & Franses, E. I. 1995 Adsorption dynamics of surfactants at the air/water interface: a critical review of mathematical models, data, and mechanisms. *Colloids and Surfaces* **100**, 1–45.

Chen, J. & Stebe, K. 1996 Marangoni retardation of the terminal velocity of a settling droplet: The role of surfactant physico-chemistry. *J. Colloid Interface Sci.* **178**, 144–155.

Chen, J. & Stebe, K. 1997 Surfactant-induced retardation of the thermocapillary migration of a droplet. *J. Fluid Mech.* **340**, 35–60.

Cuenot, B., Magnaudet, J. & Spennato, B. 1996 The effects of slightly soluble surfactants on the flow around a spherical bubble. *J. Fluid Mech.* **339**, 25–53.

Davis, R. E. & Acrivos, A. 1966 The influence of surfactants on the creeping motion of bubbles. *Chem. Engng Sci.* **21**, 681–685.

Deryagin, B. V., Dukhin, S. S. & Lisichenko, V. A. 1959 The kinetics of the attachment of mineral particles to bubbles during flotation. I. The electric field of a moving bubble *Russ. J. Phys. Chem.* **33**, 389–393.

Duineveld, P. C. 1994 Bouncing and coalesence of two bubbles in water. PhD Thesis, University of Twente, The Netherlands.

Edge, R. M. & Grant, C. D. 1972 The motion of drops in water contaminated with a surface active agent *Chem. Engng Sci.* **27**, 1709–1721.

Edwards, D. A., Brenner, H. & Wasan, D. T. 1991 *Interfacial Transport Processes and Rheology*. Butterworth-Heinemann.

Elzinga, E. R. & Banchero, J. T. 1961 Some observations on the mechanics of drops in liquid-liquid systems. *AIChE J.* **7**, 394–399.

Frumkin, A. & Levich, V. 1947 On surfactants and interfacial motion. *Zhur. Fiz. Khim.* **21**, 1183 (in Russian).

Garner, F. H. & Skelland, H. P. 1955 Some factors affecting droplet behavior in liquid-liquid systems. *Chem. Engng Sci.* **4**, 149–158.

Griffith, R. M. 1962 The effect of surfactants on the terminal velocity of drops and bubbles. *Chem. Engng Sci.* **17**, 1057–1070.

Happel, J. & Brenner, H. 1962 *Low Reynolds Number Hydrodynamics*. Prentice Hall.

Harper, J. F. 1973 On bubbles with small immobile adsorbed films rising in liquids at Low Reynolds numbers *J. Fluid Mech.* **58**, 539–545.

Harper, J. F. 1974 On spherical bubbles rising steadily in dilute surfactant solutions *Q. J. Mech. Appl. Maths* **27**, 87–100.

Harper, J. F. 1982 Surface activity and bubble motion *Appl. Sci. Res.* **38**, 343–351.

He, Z., Maldarelli, C. & Dagan, Z. 1991 The size of stagnant caps of bulk soluble surfactant on the interfaces of translating fluid droplets. *J. Colloid Interface Sci.* **146**, 442–451.

Holbrook, J. A. & Levan, M. D. 1983*a* Retardation of droplet motion by surfactant. Part I. Theoretical development and asymptotic solutions. *Chem. Engng Commun.* **20**, 191–207.

Holbrook, J. A. & Levan, M. D. 1983*b* Retardation of droplet motion by surfactant. Part II. Numerical solutions for exterior diffusion, surface diffusion, and adsorption kinetics. *Chem. Engng Commun.* **20**, 273–290.

Horton, T. J., Fritsch, T. R. & Kintner, R. C. 1965 Experimental determination of circulation velocities inside drops. *Can. J. Chem. Engng* **43**, 143–146.

Huang, W. S. & Kintner, R. C. 1969 Effects of surfactants on mass transfer inside drops. *AIChE J.* **15**, 735–744.

https://doi.org/10.1017/S0022112099005157 Published online by Cambridge University Press

Kim, H. & Subramanian, R. 1989*a* Thermocapillary migration of a droplet with insoluble surfactant, I. Surfactant cap. *J. Colloid Interface Sci.* **127**, 417–430.

Kim, H. & Subramanian, R. 1989*b* Thermocapillary migration of a droplet with insoluble surfactant, II. General case *J. Colloid Interface Sci.* **130**, 112–125.

Leppinen, D. M., Renksizbulut, M. & Haywood, R. J. 1996*a* The effects of surfactants on droplet behaviour at intermediate Reynolds numbers – I. The numerical model and steady-state results. *Chem. Engng Sci.* **51**, 479–489.

Leppinen, D. M., Renksizbulut, M. & Haywood, R.J. 1996*b* The effects of surfactants on droplet behaviour at intermediate Reynolds numbers – II. Transient deformation and evaporation. *Chem. Engng Sci.* **51**, 491–501.

Levan, M. & Newman, J. 1976 The effect of surfactant on the terminal and interfacial velocities of a bubble or drop. *AIChE J.* **22**, 695–701.

Levich, V. G. 1962 *Physicochemical Hydrodynamics.* Prentice Hall.

Masliyah, J. H. & Epstein, N. 1971 Numerical solution of heat and mass transfer from spheroids in steady axisymmetric flow. *Prog. Heat Mass Transfer* **6**, 613–632.

McLaughlin, J. B. 1996 Numerical simulation of bubble motion in water. *J. Colloid Interface Sci.* **184**, 614–625.

Nadim, A. & Borhan, A. 1989 The effects of surfactant on the motion and deformation of a droplet in thermocapillary migration. *PhysicoChem. Hydrodyn.* **11**, 753–764.

Peyret, R. & Taylor, T. D. 1983 *Computational Methods for Fluid Flow*. Springer.

Ryskin, G. & Leal, L. G. 1982 Numerical solution of free-boundary problems in fluid mechanics. *J. Fluid Mech.* **148**, 1–17.

Sadhal, S. & Johnson, R. 1982 Stokes flow past bubbles and drops partially coated with thin films. Part 1. Stagnant cap of surfactant film – exact solution *J. Fluid Mech.* **126**, 237–250.

Savic, P. 1953 Circulation and distortion of liquid drops falling through a viscous medium. *Natl Res. Counc. Can., Div. Mech. Engng Rep.* MT-22.

Saville, D. 1973 The effects of interfacial tension on the motion of drops and bubbles. *Chem. Engng J.* **5**, 251–259.

Stebe, K. J., Lin, S.-Y. & Maldarelli, C. 1991 Remobilizing surfactant retarded fluid particle interfaces. I. Stress-free conditions at the interfaces of micellar solutions of surfactants with fast sorption kinetics. *Phys. Fluids* A **3**, 3–20.

Yamamoto, T. & Ishii, T. 1987 Effect of surface active materials on the drag coefficients and shapes of single large gas bubbles. *Chem. Engng Sci.* **42**, 1297–1303.

https://doi.org/10.1017/S0022112099005157 Published online by Cambridge University Press